Organic guests inclusion by tungsten-calix[4]arene hosts†

Arturo Arduini,[a] Chiara Massera,[b] Andrea Pochini,*[a] Andrea Secchi[a] and Franco Ugozzoli*[b]

Received (in Montpellier, France) 1st March 2006, Accepted 6th April 2006
First published as an Advance Article on the web 2nd May 2006
DOI: 10.1039/b603006h

The binding mode of a series of lower rim tungsten-calix[4]arenes toward different neutral organic guests has been investigated in the solid state and through *ab initio* computational studies. From the structure of the inclusion compounds examined it emerges that the metal can be employed as a control element to confer different *cone* shapes to the calixarene cavity and to act as an additional binding site.

Introduction

Calix[4]arenes possess a π-donor cavity suitable to bind, through weak host guest CH···π interactions, small organic guests bearing acid CH groups.[1] From the extensive investigations carried out during the last few decades to single out the parameters that govern their binding efficiency, it emerged that the increase of the host rigidity strongly enhances the binding efficiency of the calixarene cavity.[1a,c] The macrocycle skeleton can be blocked in a rigid *cone* conformation by connecting its proximal phenolic OH groups with two short diethyleneglycol chains[2] or, alternatively, through the partial functionalization of the lower rim with alkyl chains.[3] By this way the host is able to act as a monotopic receptor. A further and substantial increase of binding efficiency can be gained by using heteroditopic calix[4]arene-based hosts, obtained by inserting an additional binding site onto the upper rim of the calixarene.[4]

A complementary strategy to insert additional binding sites is represented by the studies carried out by Reinaud and co-workers who exploited calix[6]arene derivatives characterised by the presence of a transition metal centre anchored at the lower rim.[5] The binding properties of these heteroditopic hosts clearly demonstrated that this arrangement of binding sites can result in hosts endowed with new and fascinating properties.

In this context, the ability of calix[4]arenes bearing transition metals covalently linked at the lower rim phenolic oxygens, to act as heteroditopic hosts, remains relatively unexplored. In fact, despite the rich literature reported so far on this type of metalla-calix[4]arenes,[6] most of the studies have mainly been devoted to revealing the properties of the metal centre, considering the calix[4]arene as a new ligand for the metal. Among the transition metals employed, tungsten-based calix[4]arenes have been extensively studied.[7] Thus, it appeared to us that this class of calix[4]arene derivatives could represent a suitable tool to investigate the use of metal centres to control the shape of the calixarene cavity and to study the role of the metal as an additional binding site.

Herewith we present an investigation based on X-ray crystallographic data and *ab initio* calculations on the complexation properties of a series of calix[4]arene derivatives blocked in a rigid *cone* conformation by a tungsten(VI) metal centre, toward neutral organic guests.

Results and discussion

Design and synthesis of the hosts

Among the tungsten-calix[4]arenes that have been reported so far in the literature, we selected two series of compounds that are both characterised by the metal bonded to the four calixarene oxygens. In one series, the metal is hexo-cavity bonded through two other oxygens of a pyrocatechol unit, while in the other, the tungsten is in its oxo form.[6c,7a] Calix[4]arenes (**1a–c**), characterised by the presence of different substituents onto their *para* position, were employed for the host synthesis. Tungsten(VI) pyrocatechol calix[4]arenes (**3a–c**) were prepared in 65–85% overall yield, (see Scheme 1) by modifying the synthetic procedure devised by Swager and co-workers.[7b,c] The series of tungsten(VI) oxo hosts (**4a–c**)[8] was prepared adapting the procedure published by Floriani and co-workers.[7a] According to this latter synthesis, in hosts (**4a–c**) a molecule of acetic acid is included inside the calixarene cavity to "saturate" the coordination sphere of the metal.

The structures of the new compounds **3a–c** and **4c** were inferred through spectroscopic techniques (see Experimental). Particularly informative was the observation that in the ^{1}H NMR spectra, all the tungsten(VI) pyrocatechol calix[4]arene derivatives **3a–c** adopt a distorted *cone* conformation having a C_{2v} symmetry. This was clearly evidenced by the two sets of signals for the aromatic and *tert*-butyl or cyclohexyl groups present on the *para* position of the aromatic rings of **3b** and **3c**, respectively. On the contrary, compound **4c** assumes a *cone* conformation, having a C_{4v} symmetry, as showed by the presence of one singlet for the four equivalent aromatic protons and by a unique set of resonances for the cyclohexyl moiety in its ^{1}H NMR spectrum.[9]

[a] *Dipartimento di Chimica Organica e Industriale, Università di Parma, via G.P. Usberti 17/a, I-43100, Italy. Fax: +39 0521 905472*
[b] *Dipartimento di Chimica Generale ed Inorganica, Chimica Analtica, Chimica Fisica, Università di Parma, via G.P. Usberti 17/a, I-43100, Italy. E-mail: ugoz@unipr.it; Fax: +39 0521 905557; Tel: +39 0521 905417*

† Electronic supplementary information (ESI) available: Interaction energies in the benzene/acetone complex as a function of the H···C_t distance (C_t = benzene centroid) calculated with the cc-PVDZ and cc-PVTZ basis sets. See DOI: 10.1039/b603006h

Solid state complexation studies

The ability of **3a–c** and **4a–c** to behave as hosts was evaluated toward a series of small neutral organic molecules representative of different classes of Volatile Organic Compounds (VOCs), able to interact with both the π-donor cavity and the metal centre. The guests used were: ethyl acetate, acetone, acetonitrile, and *N,N*-dimethyl formamide. As a working hypothesis the calix[4]arenes **3a–c**, where the tungsten(VI) core is fully coordinated by six oxygen atoms, should experience a binding mode related to that of rigid calix[4]arenes,[2] and thus able to interact with the guest only through the aromatic cavity. On the contrary, in **4a–c**, the metal, although hexacoordinated, presents a ligand (acetic acid) inside the cavity that could be exchanged. This could allow a different ligand (guest) to be recognised by a combination of weak (through the cavity) and stronger coordinative (through the metal) intermolecular interactions.

Unfortunately, all attempts to obtain crystals of the tungsten(VI) oxo calix[4]arene hosts **4a–c**, with the different guests failed. However, when compounds **3a–c** were used as hosts, crystals suitable for X-ray crystallographic determination of the corresponding inclusion complexes were obtained from the slow evaporation of CH_2Cl_2 solutions of **3a** (R = H) with DMF and ethyl acetate, **3b** (R = ^{t}Bu) with acetone, and **3c** (R = cyclohexyl) with acetonitrile. Quite surprisingly, NMR analysis of the crystals showed that only in the complex with acetone (acetone ⊂ **3b**) does the host retain its original structure. On the contrary, the formation of tungsten(VI) oxo calix[4]arene derivatives was observed with more strongly coordinating guests (see Scheme 1), and the following inclusion complexes DMF ⊂ **4a**, H_2O/AcOEt ⊂ **4a**, and CH_3CN ⊂ **4c** were isolated.[10]

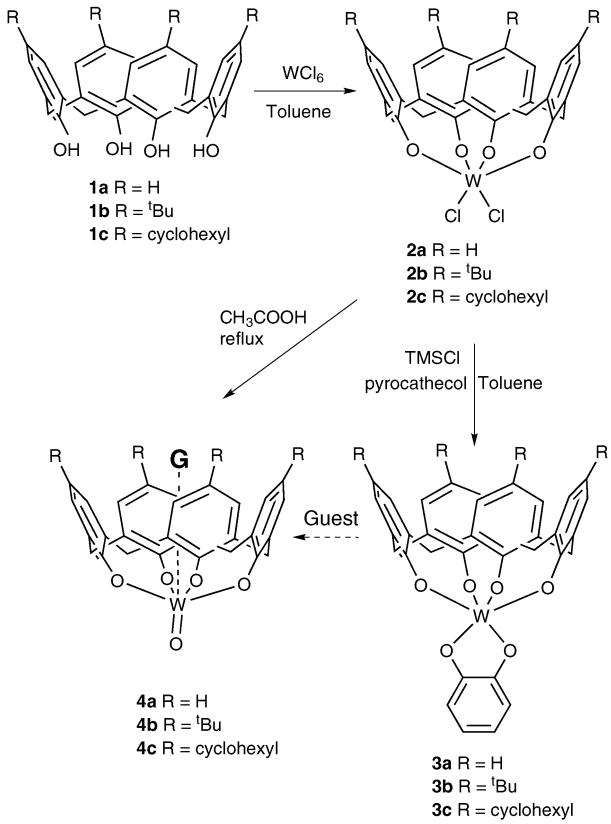

Scheme 1

X-Ray studies

As far as the shape of the host is concerned, complex acetone ⊂ **3b** adopts a highly *flattened cone* conformation, as found for instance in the structure of the complex benzene ⊂ **2b**.[7a] In DMF ⊂ **4a** the host conformation is *flattened*, whereas in H_2O/AcOEt ⊂ **4a** and in CH_3CN ⊂ **4c** the host assumes a "slightly distorted" and an "ideal" *cone* conformation, respectively. The quantitative and unequivocal description of the molecular conformation of the host in the four complexes is summarised in Table 1 by the dihedral angles δ, calculated according to the standard rules,[11] and by the conformational parameters φ and χ and the *symbolic representations*.[12]

In acetone ⊂ **3b** (see Fig. 1), contrary to what is expected, the guest molecule does not enter inside the cavity with its oxygen atom, but it prefers to fill the host cavity with the two methyl groups. This reciprocal host–guest orientation allows the activation of three (not equivalent) attractive CH···π interactions between the "acid" hydrogen atoms of the two methyl groups of the acetone and the electron rich aromatic nuclei of the host as shown in Fig. 1.[13] The shortest H···C_tD (C_t = ring centroid) separation of 2.77(1) Å (see Table 2) is indicative of a strong CH···π interaction with the aromatic ring D, while the other two acetone/aromatic separations, H···C_tB 2.83(1) Å and H···C_tC 2.81(1) Å, are practically identical to each other but longer. To clarify whether these

Table 1 Dihedral angles[a] δ (°) and conformational parameters[b] φ and χ (°) in complexes acetone ⊂ **3b**, CH_3CN ⊂ **4c**, DMF ⊂ **4a** and H_2O/AcOEt ⊂ **4a**

					A–B		B–C		C–D		D–A	
Complex	R ^ A	R ^ B	R ^ C	R ^ D	φ	χ	φ	χ	φ	χ	φ	χ
Acetone ⊂ **3b**												
	146.6(3)	116.9(2)	158.4(2)	117.9(3)	113(1)	−84(1)	82(1)	−122(1)	125(1)	−85(1)	82(1)	−112(1)
CH_3CN ⊂ **4c**	127.5(2)	127.5(2)	127.5(2)	127.5(2)	94.2(9)	−93.7(9)	94.2(9)	−93.7(9)	94.2(9)	−93.7(9)	94.2(9)	−93.7(9)
DMF ⊂ **4a**	117.1(1)	127.0(2)	117.1(2)	131.2(2)	82.9(7)	−90.1(8)	89.4(7)	−83.8(8)	83.9(7)	−93.0(7)	92.5(8)	−82.0(8)
H_2O/AcOEt ⊂ **4a**	123.8(2)	124.9(2)	125.4(2)	123.8(2)	89.9(9)	−88.1(9)	89.1(9)	−88.9(8)	90.2(7)	−88.4(7)	89.2(8)	−87.9(8)

[a] Dihedral angles between the molecular reference plane R (the weighted least-squares plane through the four CH_2 bridges) and the weighted least-squares planes of the phenolic rings (A, B, C, D). [b] The *symbolic representations* of the molecular conformations are: C_1 +−, +−, +−, +−, for acetone ⊂ **3b**, DMF ⊂ **4a**, H_2O/AcOEt ⊂ **4a**, and C_4 +− for CH_3CN ⊂ **4c**, respectively.

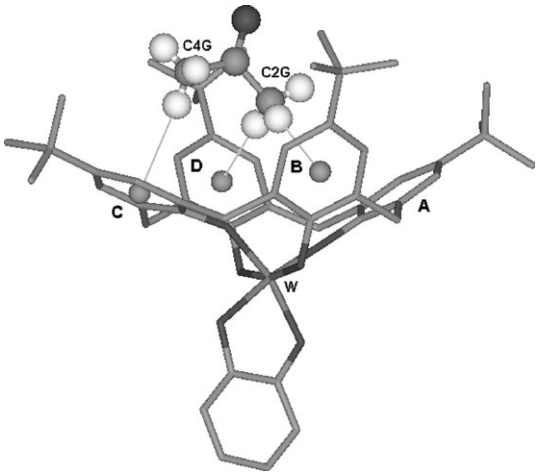

Fig. 1 Partial stick view of acetone ⊂ **3b**.The host is represented in stick mode; the guest in ball and stick mode. Only the hydrogen atoms of the guest have been drawn. CH···π interactions are shown by fine lines.

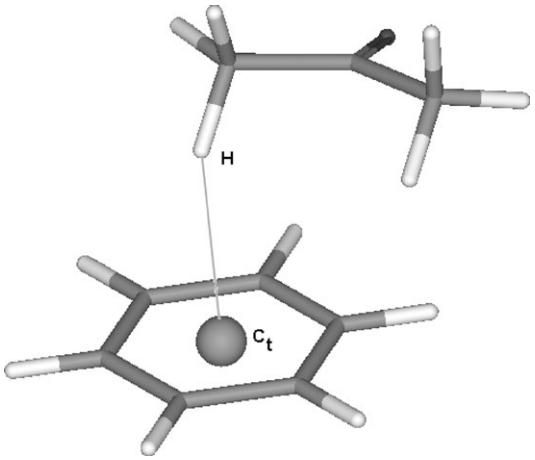

Fig. 2 Optimised geometry of the acetone–benzene complex in the gas-phase.

latter short contacts can be considered true CH···π interactions and in general to evaluate the binding energy between the "acid" hydrogens of acetone and the electron-rich surface of benzene, we carried out *ab initio* calculations of the intermolecular interaction energy when an isolated molecule of acetone approaches a benzene molecule.

Initially, we calculated the minimum-energy structure of the complex at the MP2/cc-PVDZ level (see Fig. 2). In a second step, starting from the obtained equilibrium geometry, we carried out the calculation of the interaction energies as a function of H···C_t separations in the range 2.2 ≤ H···C_t ≤ 4.4 Å at the MP2 level using both cc-PVDZ and cc-PVTZ basis sets (see ESI† for the calculation details). The plot of the interaction energies (see Fig. 3) shows that the small cc-PVDZ basis set underestimates the attraction compared to larger cc-PVTZ, because the former leads to an underestimate of the molecular polarizability and the dispersion interactions. The energy minimum is found at H···C_t = 2.6 Å with the cc-PVDZ basis set and at 2.8 Å with the larger cc-PVTZ set. The angle between the C═O dipole and the benzene ring is 16.8°. However, the energy of binding estimated using cc-PVTZ (E_{MP2} = −17.54 kJ mol^{-1}) is 54% higher than that calculated with cc-PVDZ (E_{MP2} = −11.4 kJ mol^{-1}). The large gain of attraction by electron correlation [E_{corr} = E_{MP2} − E_{HF} is −20.74 kJ mol^{-1} (cc-PVTZ) against –14.55 kJ mol^{-1} (cc-PVDZ)] indicates that dispersion is significantly important for attraction in the CH···π interaction between these two fragments. From the plot of the interaction energies it is also evident that (a) the attraction is still substantial up to 3.0 Å, where the binding energy is comparable (E_{MP2} = −15.93 kJ mol^{-1}), and (b) in any case the interaction energy profile is almost flat around the minimum from 2.6 Å (E_{MP2} = −17.46 kJ mol^{-1}) to 3.0 Å (E_{MP2} = −15.93 kJ mol^{-1}).

These results help to conclude that, in the structure of acetone ⊂ **3b**, the three acetone–aromatic interactions, for which the H···C_t distances range from to 2.77 to 2.83 Å, are not only all true CH···π interactions, but they are also practically equivalent from the energetic point of view. It is noteworthy that the orientation of the C═O dipole of acetone with aromatic rings are 19.2, 32.4, and 82.6° for rings D, B and C, respectively, so that the strongest CH···π interaction (with

Table 2 Geometrical parameters for CH···π and OH···π interactions in acetone ⊂ **3b**, DMF ⊂ **4a** and H_2O/AcOEt ⊂ **4a**[a]

Complex	D–H···A[b]	C···C_t/Å	H···C_t/Å	C–H···C_t/°
Acetone ⊂ **3b**	C2G–H···C_tB	3.78(1)	2.83(1)	171(1)
	C2G–H···C_tD	3.72(1)	2.77(1)	171(1)
	C4G–H···C_tC	3.60(1)	2.81(1)	140(1)
DMF ⊂ **4a**	C1G–H···C_tB	3.190(8)	2.363(8)	154.2(7)
	C2G–H···C_tD	3.321(9)	2.661(8)	139.9(7)
		O···C_t/Å	**H···C_t/Å**	**O–H···C_t/°**
H_2O/AcOEt ⊂ **4a**	Ow–H···C_tB	3.42(1)	2.69(1)	132.5(8)
	Ow–H···C_tD	3.43(1)	2.63(1)	141.8(8)

[a] C_t = centroid. [b] D = donor, A = acceptor.

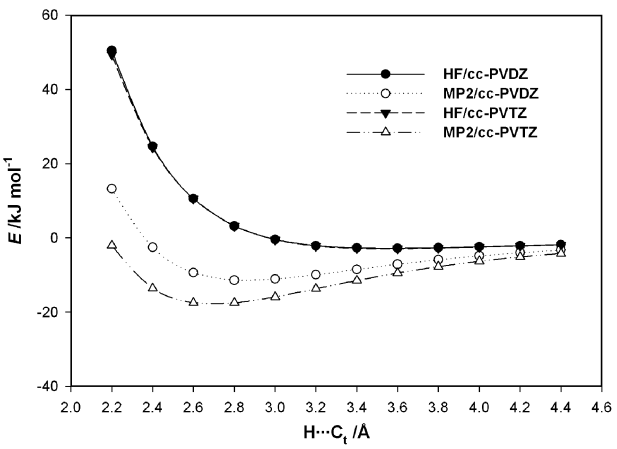

Fig. 3 HF and MP2 interaction energies (kJ mol^{-1}), calculated with the cc-PVDZ and cc-PVTZ basis sets, for rigid relative translations of monomers starting from the equilibrium geometry of the acetone–benzene complex.

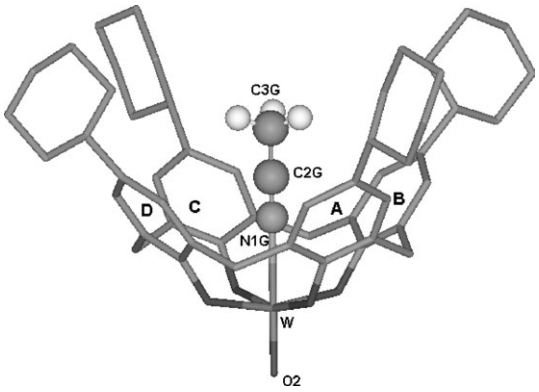

Fig. 4 Partial stick view of $CH_3CN \subset$ **4c**. The host is represented in stick mode; the guest in ball and stick mode. Only one of the four different orientations of the hydrogen atoms of the guest has been drawn.

ring D) occurs at an angle close to that found in the acetone–benzene complex (16.8°).

In $CH_3CN \subset$ **4c** the host has a C_4 symmetry, and the nitrogen of the guest is bonded to the metal, with a N···W bond length of 2.328(10) Å,[14] and lies on the fourfold axis with the methyl group disordered over four different equivalent orientations around the C_4 axis (see Fig. 4). Apart from van der Waals interactions, no other weak intermolecular interactions occur between the host and the guest.[15]

In DMF $\subset$ **4a** (see Fig. 5) the guest is held within the calixarene cavity through its oxygen atom (O1G) coordinated to the metal centre [W···O1G 2.310(4) Å]. The final orientation of the guest within the cavity is then adjusted by simple rotation of the guest itself around the bond O1G–W to bring the CH hydrogen and one methyl hydrogen of the guest to interact with the electron-rich surfaces of the two opposite phenolic rings B and D giving rise to two attractive CH···π interactions.

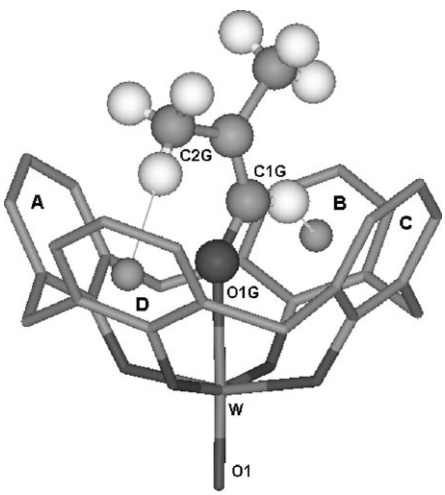

Fig. 5 Partial stick view of DMF $\subset$ **4a**. The host is represented in stick mode; the guest in ball and stick mode. Only the hydrogen atoms of the guest have been drawn. CH···π interactions and hydrogen bonds are shown by fine lines.

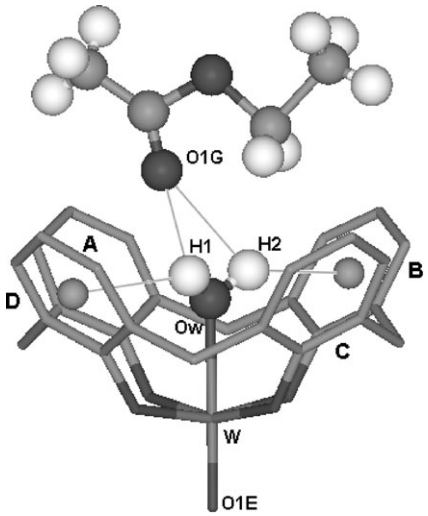

Fig. 6 Partial stick view of H_2O/AcOEt $\subset$ **4a**. The host is represented in stick mode; the guest in ball and stick mode. Only the hydrogen atoms of the guest have been reported. CH···π interactions and hydrogen bonds are shown by fine lines.

In H_2O/AcOEt $\subset$ **4a** (see Fig. 6) one water molecule, directly coordinated to the metal centre [W···Ow 2.331(4) Å], is further stabilised within the calixarene cavity by two OH···π interactions with the two opposite phenolic rings B and D (the water molecule can adjust its orientation within the cavity by a rigid rotation around the W–O_W bond).

The H···C_t separations of 2.63(1) and 2.69(1) Å (see Table 2) are only slightly longer than those (2.38 and 2.5 Å) observed in the first example of a OH···π interaction between a water molecule and the calix[4]arene cavity[16] but short enough to ensure that the OH···π interaction is still attractive. One ethyl acetate molecule acts as a "second coordination sphere" ligand in the complex. Although located outside the calixarene cavity, the ethyl acetate is still linked by strong mutual attraction with the coordinated water molecule in the calixarene cavity: the $O_{C=O}$ of the ethyl acetate acts as an acceptor of two strong hydrogen bonds from the water molecule. The geometrical parameters for hydrogen bonds are summarised in Table 3.

To the best of our knowledge only two other examples of a second sphere of coordination in metalla-calix[4]arene complexes have been reported. However, the first one is a molybdenum complex,[17] whereas the second is a tungsten calix[4]arene complex in which a disordered aniline molecule is present in the second coordination sphere.[14] This prevents any other speculation on the intermolecular interaction occurring in this latter complex.

Table 3 Geometrical parameters for hydrogen bonds in H_2O/AcOEt $\subset$ **4a**

	D···A/Å	H···A/Å	D–H···A/°
Ow–H1···O1G	2.60(1)	2.07(1)	113.6(8)
Ow–H2···O1G	2.60(1)	2.62(1)	78.5(8)

Conclusions

These results clearly demonstrate that a transition metal centre, anchored to the lower rim of a calix[4]arene platform, can act as an efficient preorganising element. The guest can be covalently bound to the metal centre within the host cavity without any other interactions with the host as for the CH_3CN molecule in $CH_3CN \subset$ **4c**.

The guest can be linked to the host through cooperatively strong and weak interactions. The guest can be primarily covalently linked to the metal centre within the host cavity and then anchored in to the walls of the host by using multiple CH$\cdots\pi$ interactions such as for the DMF molecule in DMF $\subset$ **4a**. Again, a guest can be linked to another guest directly coordinated to the metal centre within the cavity giving rise to a "secondary coordination sphere" to the metal. This is the case for the AcOEt molecule which is linked through hydrogen bonds to a water molecule coordinated to the tungsten centre within the cavity as in H_2O/AcOEt $\subset$ **4a**. Finally, the metal centre can be used to force a very flattened *cone* conformation of the calixarene to exploit the inner aromatic surfaces of the calix[4]arene for CH$\cdots\pi$ interactions with selected guests which can afford new interaction modes with the aromatic cavity as verified in acetone $\subset$ **3b**.

Experimental

Materials and methods

All reactions were carried out under nitrogen, and all solvents were freshly distilled under nitrogen prior to use. All other reagents were reagent grade quality obtained from commercial supplies and used without further purification. ^{1}H NMR spectra were recorded at 300 and 400 MHz. ^{13}C NMR were recorded at 25 and 75 MHz. Chemical shifts (δ) are expressed in ppm from the solvent residual signal. Mass spectra were recorded in the CI mode (CH_4). Compounds **1a**,[18] **1b**[19] and **1c**[20] were synthesised according to literature procedures.

General procedure for the synthesis of compounds 3a–3c

To a purple suspension of WCl_6 (0.4 g, 1 mmol) in dry toluene (15 mL), the appropriate calix[4]arene **1a–c** (1 mmol) was added. The resulting heterogeneous mixture was stirred at room temperature for 24 h, then pyrocatechol (0.1 g, 1 mmol) and $(CH_3)_3SiCl$ (0.2 g, 2 mmol) were added. The mixture was refluxed under stirring for 6–12 h, after which it was cooled at room temperature and filtered.

Compound 3a. The filtrate was evaporated to dryness under reduced pressure to afford 0.5 g (65%) of a red solid residue which did not require further purification (Found: C, 55.8; H, 3.7. $C_{34}H_{24}O_6W$ requires C, 57.3; H, 3.4%). mp $>$ 300 °C (from toluene). δ_H ($CDCl_3$, 300 MHz): 3.43 (4H, d, J_{AX} 12, ArCH_2Ar equatorial), 4.66 (4H, d, J_{AX} 12, ArCH_2Ar axial), 6.65 (2H, t, J 7.5, Ar–H), 6.90 (2H, t, J 7.3, Ar–H), 6.95 (4H, bs, Ar–H), 7.05 (4H, d, J 7.5, Ar–H), 7.26 (4H, d, J 7.3, Ar–H); δ_C ($CDCl_3$, 75 MHz): 29.7, 115.5, 123.8, 124.7, 125.3, 126.6, 129.8, 130.0, 136.1, 156.3, 158.6, 163.4; m/z (CI) 713 (MH^+).

Compound 3b. The filtrate was evaporated to dryness under reduced pressure to afford a red solid residue which was taken up with ethyl acetate and filtered on Celite. Evaporation of the filtrate yielded 0.8 g (84%) of a red solid compound (Found: C, 63.0; H, 6.2. $C_{50}H_{56}O_6W$ requires C, 64.1; H, 6.0%). mp $>$ 300 °C (from ethyl acetate). δ_H ($CDCl_3$, 300 MHz): 1.18 (18H, s, –C(CH_3)$_3$), 1.37 (18H, s, –C(CH_3)$_3$), 3.39 (4H, d, J_{AX} 12, ArCH_2Ar equatorial), 4.66 (4H, d, J_{AX} 12, ArCH_2Ar axial), 6.82 and 6.85 (4H, 2s, Ar–H), 6.91 and 7.06 (8H, 2t, Ar–H); δ_C ($CDCl_3$, 75 MHz): 31.4, 31.8, 33.9, 34.4, 34.7, 115.3, 123.6, 124.2, 125.9, 126.7, 129.7, 135.5, 145.8, 148.5, 156.5, 161.4; m/z (CI) 937 (MH^+).

Compound 3c. The filtrate was evaporated to dryness under reduced pressure to afford a red solid residue which was crystallised from ethyl acetate to yield 0.9 g (86%) of a red solid compound (Found: C, 66.2; H, 6.3. $C_{58}H_{64}O_6W$ requires C, 66.9; H, 6.2%). mp $>$ 300 °C (from ethyl acetate). δ_H ($CDCl_3$, 300 MHz): 1.2–1.5 and 1.6–1.9 (40H, 2m, cyclohexyl), 2.35 and 2.55 (4H, 2bs, cyclohexyl), 3.35 (4H, d, J_{AX} 13.5, ArCH_2Ar equatorial), 4.62 (4H, d, J_{AX} 13.5, ArCH_2Ar axial), 6.87 (4H, bs, Ar–H), 6.92 and 7.08 (8H, 2t, Ar–H); δ_C ($CDCl_3$, 75 MHz): 26.1, 26.8, 26.9, 29.6, 33.9, 34.5, 34.9, 43.2, 43.5, 44.4, 115.5, 124.2, 124.9, 128.0, 129.7, 135.9, 142.7, 145.4, 156.4, 156.9, 161.8; m/z (CI) 1040 (MH^+).

Compound 4c. To a purple suspension of WCl_6 (0.4 g, 1 mmol) in dry toluene (15 mL), calix[4]arene **1c** (0.2 g, 0.26 mmol) was added. The resulting heterogeneous mixture was stirred at room temperature for 18 h, then evaporated to dryness under reduced pressure. The reddish solid residue was taken up with CH_3COOH (15 mL) and a catalytic amount of $AlCl_3$ was added. The mixture was refluxed under stirring for a further 6 h, after which it was cooled at room temperature and filtered to afford a yellow solid residue (0.2 g, 75%) which did not require further purification (Found: C, 66.2; H, 6.1. $C_{52}H_{60}O_5W$ requires C, 65.8; H, 6.4%). mp $>$ 300 °C (from ethyl acetate). δ_H ($CDCl_3$, 300 MHz): 1.2–1.3 (24 H, m, cyclohexyl), 1.7–1.8 (16 H, m, cyclohexyl), 2.33 (4 H, bs, cyclohexyl), 3.24 (4H, d, J_{AX} 12.6, ArCH_2Ar equatorial), 4.65 (4H, d, J_{AX} 12.6, ArCH_2Ar axial), 6.93 (8H, s, Ar–H); δ_C ($CDCl_3$, 75 MHz): 26.0, 26.8, 32.7, 34.6, 43.7, 44.4, 126.4, 124.1, 130.0; m/z (CI) 949 (MH^+).

Computational Studies

The optimised geometry of the benzene–acetone complex was obtained by *ab initio* calculations in the gas phase with the MP2 method[21] by using the cc-PVDZ[22] basis set in Gaussian 03.[23] The interaction energy pattern as a function of H$\cdots$C$_t$ distance was obtained by single point calculations with the MP2 method using the cc-PVDZ and cc-PVTZ[24] basis sets, by increasing step by step (0.2 Å) the H$\cdots$C$_t$ distance from 2.2 to 4.4 Å in the optimised structure of the complex and fixing any other geometrical parameters. The calculated energy values were corrected for basis set polarization effects (BSSE).[25]

Crystallography

Data were collected at 295 K on Philips PW 1100 (DMF $\subset$ **4a** and $CH_3CN \subset$ **4c**) and on Siemens AED (acetone $\subset$ **3b** and

Table 4 Crystal data and experimental details for data collection and structure refinement for acetone ⊂ **3b**, CH_3CN ⊂ **4c**, DMF ⊂ **4a** and H_2O/AcOEt ⊂ **4a**

Compound	Acetone ⊂ **3b**	CH_3CN ⊂ **4c**	DMF ⊂ **4a**	H_2O/AcOEt ⊂ **4a**
Empirical Formula	$C_{44}H_{52}O_4W \cdot C_6H_4O_2 \cdot C_3H_6O$	$C_{52}H_{60}O_5W \cdot CH_3CN$	$C_{28}H_{20}O_5W \cdot C_3H_7NO$	$C_{28}H_{20}O_5W \cdot C_4H_8O_2 \cdot H_2O$
Formula weight	994.919	982.892	693.407	726.434
Crystal size/mm	0.2 × 0.3 × 0.3	0.3 × 0.4 × 0.3	0.2 × 0.2 × 0.3	0.2 × 0.4 × 0.3
Crystal system	Triclinic	Tetragonal	Monoclinic	Monoclinic
Space group	*P*-1	*P*4/*n*	$P2_1/n$	$P2_1/n$
a/Å	14.243(5)	13.292(5)	8.789(5)	11.302(5)
b/Å	17.340(5)	13.292(5)	17.600(5)	14.802(5)
c/Å	10.360(5)	13.743(5)	16.397(5)	17.226(5)
α/°	90.99(1)	90	90	90
β/°	102.51(1)	90	94.94(1)	91.05(1)
γ/°	98.44(1)	90	90	90
V/Å^3	2468(2)	2428(2)	2527(2)	2881(2)
Z	2	2	4	4
ρ (calcd.)/g cm^{-3}	1.339	1.344	1.823	1.675
F (000)	1020	1002	1368	1440
T/K	295	295	295	295
λ/Å	0.710 73	0.710 73	0.710 73	0.710 73
μ/mm^{-1}	2.389	2.424	4.620	4.06
Index ranges	$-16 \le h \le 16$ $-20 \le k \le 19$ $-2 \le l \le 12$	$-14 \le h \le 14$ $0 \le k \le 14$ $0 \le l \le 14$	$-14 \le h \le 14$ $0 \le k \le 28$ $0 \le l \le 26$	$-12 \le h \le 10$ $-15 \le k \le 16$ $-19 \le l \le 13$
Reflections collected	9236	3288	11 745	4893
Independent. Reflections	8695	1490	11 083	4510
R_{int}	0.034	0.059	0.025	0.030
Observed Reflections	5339 $F_o \ge 4\sigma(F_o)$	1075 $F_o \ge 4\sigma(F_o)$	5990 $F_o \ge 4\sigma(F_o)$	2845 $F_o \ge 4\sigma(F_o)$
Parameters/restraints	562/24	146/0	358/0	383/3
R_1[a]	0.0825	0.0402	0.0670	0.0303
wR_2	0.2154	0.0995	0.1801	0.0689
Goodness-of-fit[b]	0.913	0.780	0.857	0.843

[a] $R_1 = \Sigma\|F_o| - |F_c\|/\Sigma|F_o|$, $wR_2 = [\Sigma w(F_o^2 - F_c^2)^2/\Sigma wF_o^4]^{1/2}$. [b] Goodness-of-fit = $[\Sigma w(F_o^2 - F_c^2)^2/(n-p)]^{1/2}$, where *n* is the number of reflections and *p* is the number of parameters.

H_2O/AcOEt ⊂ **4a**) diffractometers using graphite-monochromated Mo-Kα radiation (*λ* = 0.710 73 Å). Crystal data and relevant experimental details are presented in Table 4. For each complex the cell parameters were obtained by a least-squares fit of 30 $I(\theta,\kappa,\phi)_{hkl}$ reflections found in a random search on the reciprocal lattice. Diffraction data were corrected for Lorentz and polarization effects. Absorption correction was applied using ABSORB[26] at the end of the isotropic refinement. The structures were solved by direct methods using SIR92[27] and refined by full matrix least-squares on F^2 with SHELX-97[28] using anisotropic atomic displacements for all non-hydrogen atoms except the carbon atoms of the *tert*-butyl group on the phenolic rings A and D in acetone ⊂ **3b**, which were disordered over two different orientations, and for which isotropic atomic displacements were used. Generally the hydrogen atoms were placed in their calculated position with the geometrical constraint C–H = 0.96 Å and refined with isotropic atomic displacements "riding" on their parent atoms. The two water hydrogens in H_2O/AcOEt ⊂ **4a** were found in the Fourier Δ*F* map and refined with isotropic atomic displacements. All the geometrical calculations were obtained by PARST97.[29]

CCDC reference numbers 299163 (acetone ⊂ **3b**), 299164 (DMF ⊂ **4a**), 299165 (CH_3CN ⊂ **4c**), and 299166 (H_2O/AcOEt ⊂ **4a**).

For crystallographic data in CIF or other electronic format see DOI: 10.1039/b603006h

Acknowledgements

This research was partly supported by FIRB (Manipolazione Molecolare per Macchine Nanometriche), MIUR "Supramolecular Devices Project". Authors thank Centro Interdipartimentale di Misure "G. Casnati" for NMR measurements.

References

1 See *e.g.*: (*a*) A. Arduini and A. Pochini, in *Calixarenes in Action*, ed. L. Mandolini, R. Ungaro, Imperial College Press, London, 2000, pp. 37–61; (*b*) F. Ugozzoli, in *ibid.*, pp. 145–171; (*c*) A. Arduini, A. Pochini, A. Secchi and F. Ugozzoli, in *Calixarenes*, 2001, ed. Z. Asfari, V. Böhmer, J. Harrowfield, J. Vicens, Kluwer, Dordrecht, 2001, pp. 457–475, and references therein.
2 (*a*) A. Arduini, M. Fabbi, M. Mantovani, L. Mirone, A. Pochini, A. Secchi and R. Ungaro, *J. Org. Chem.*, 1995, **60**, 1454; (*b*) A. Arduini, W. M. McGregor, D. Paganuzzi, A. Pochini, A. Secchi, F. Ugozzoli and R. Ungaro, *J. Chem. Soc., Perkin Trans. 2*, 1996, 839.
3 S. Smirnov, V. Sidorov, E. Pinkhassik, J. Havlicek and I. Stibor, *Supramol. Chem.*, 1997, **8**, 187.
4 See *e.g.*: (*a*) A. Arduini, E. Brindani, G. Giorgi, A. Pochini and A. Secchi, *J. Org. Chem.*, 2002, **67**, 6188; (*b*) A. Arduini, E. Brindani, G. Giorgi, A. Pochini and A. Secchi, *Tetrahedron*, 2003, **59**, 7587.
5 (*a*) O. Sénèque, M.-N. Rager, M. Giorgi and O. Reinaud, *J. Am. Chem. Soc.*, 2000, **122**, 6183; (*b*) Y. Rondolez, M.-N. Rager, A. Duprat and O. Reinaud, *J. Am. Chem. Soc.*, 2002, **124**, 1334; (*c*) U. Daborst, M.-N. Rager, S. Petit, I. Jabin and O. Reinaud, *J. Am. Chem. Soc.*, 2005, **127**, 8517.
6 See *e.g.*: (*a*) C. Wieser, C. B. Dieleman and D. Matt, *Coord. Chem. Rev.*, 1997, **165**, 93; (*b*) J. W. Canary, B. C. Gibb, in *Progress in*

Inorganic Chemistry, ed. K. D. Karlin, John Wiley & Sons, New York, 1997, vol. 45, pp. 1–82; (*c*) C. Floriani, R. Floriani-Moro, in *Advanced in Organometallic Chemistry*, ed. R. West, A. F. Hill, Academic Press, San Diego, 2001, vol. 47, pp. 167–233, and references therein.

7 See *e.g.*: (*a*) F. Corazza, C. Floriani, A. Chiesi-Villa and C. Rizzoli, *Inorg. Chem.*, 1991, **30**, 4465; (*b*) B. Xu, Y.-J. Miao and T. M. Swager, *J. Org. Chem.*, 1998, **63**, 8356; (*c*) A. Vigalok, Z. Zhu and T. M. Swager, *J. Am. Chem. Soc.*, 2001, **123**, 7917; (*d*) A. Vigalok and T. M. Swager, *Adv. Mater.*, 2002, **14**, 368.

8 Only the *p*-cyclohexyl-substituted derivative **4c** is a new compound and was obtained in 90% of overall yield.

9 Tungsten(IV)-oxo derivatives **4a**,**b** experience very low solubility in chlorinated solvents.

10 The mechanism of these structural rearrangements at the metal centre was not studied. Nevertheless, it can be explained considering that in all the crystallisation experiments carried out, adventitious water was present.

11 M. Perrin and D. Oehler, in *Calixarenes. A Versatile Class of Macrocyclic Compounds*, ed. J. Vicens, V. Böhmer, Kluwer Academic Publishers, Dordrecht, The Netherlands, 1991, pp. 65–85.

12 F. Ugozzoli and G. D. Andreetti, *J. Inclusion Phenom. Mol. Recognit. Chem.*, 1992, **13**, 337.

13 In the inclusion complex between the *p-tert*-butylcalix[4]arene (**1b**) and acetone, the host aromatic cavity adopts a *cone* conformation and interacts only with one methyl group of the guest molecule, see K. A. Udachin, G. D. Enright, C. I. Ratcliffe and J. A. Ripmeester, *ChemPhysChem*, 2003, **4**, 1059.

14 This bond length is comparable to that found in other acetonitrile tungsten-calix[4]arene complexes, see P. Mongrain, J. Douville, J. Gagnon, M. Drouin, A. Decken, D. Fortin and P. D. Harvey, *Can. J. Chem.*, 2004, **82**, 1452.

15 In $CH_3CN \subset$ **4c** the guest nitrogen atom is deeply engulfed inside the cavity just above the plane R defined by the four CH_2 bridging groups [N···R distance is 0.91(1) Å]. This situation is opposite to that found in the $CH_3CN \subset$ calix[4]arene complexes stabilised only through CH···π interactions, where usually the methyl group is faced toward the aromatic cavity beneath the plane R (CH_3···R distance ranges from 2.7 to 2.8 Å). See *e.g.* A. Arduini, F. F. Nachtigall, A. Pochini, A. Secchi and F. Ugozzoli, *Supramol. Chem.*, 2000, **12**, 273, and references therein.

16 J. L. Atwood, F. Hamada, K. D. Robinson, G. W. Orr and R. L. Vincent, *Nature*, 1991, **349**, 683.

17 F. Corazza, C. Floriani, A. Chiesi-Villa and C. Guastini, *J. Chem. Soc., Chem. Commun.*, 1990, 640.

18 C. D. Gutsche and L.-G. Lin, *Tetrahedron*, 1986, **42**, 1633.

19 C. D. Gutsche and M. Iqbal, in *Organic Synthesis, Coll.*, 1993, vol.**8**, pp. 75–76.

20 A. Arduini, A. Pochini, A. Rizzi, A. R. Sicuri, F. Ugozzoli and R. Ungaro, *Tetrahedron*, 1992, **48**, 905.

21 C. Møller and M. Plesset, *Phys. Rev.*, 1934, **46**, 618.

22 D. E. Woon and T. H. Dunning Jr, *J. Chem. Phys.*, 1993, **98**, 1358.

23 M. J. Frisch, G. W. Trucks, H. B. Schlegel, G. E. Scuseria, M. A. Robb, J. R. Cheeseman, J. A. Montgomery Jr, T. Vreven, K. N. Kudin, J. C. Burant, J. M. Millam, S. S. Iyengar, J. Tomasi, V. Barone, B. Mennucci, M. Cossi, G. Scalmani, N. Rega, G. A. Petersson, H. Nakatsuji, M. Hada, M. Ehara, K. Toyota, R. Fukuda, J. Hasegawa, M. Ishida, T. Nakajima, Y. Honda, O. Kitao, H. Nakai, M. Klene, X. Li, J. E. Knox, H. P. Hratchian, J. B. Cross, V. Bakken, C. Adamo, J. Jaramillo, R. Gomperts, R. E. Stratmann, O. Yazyev, A. J. Austin, R. Cammi, C. Pomelli, J. W. Ochterski, P. Y. Ayala, K. Morokuma, G. A. Voth, P. Salvador, J. J. Dannenberg, V. G. Zakrzewski, S. Dapprich, A. D. Daniels, M. C. Strain, O. Farkas, D. K. Malick, A. D. Rabuck, K. Raghavachari, J. B. Foresman, J. V. Ortiz, Q. Cui, A. G. Baboul, S. Clifford, J. Cioslowski, B. B. Stefanov, G. Liu, A. Liashenko, P. Piskorz, I. Komaromi, R. L. Martin, D. J. Fox, T. Keith, M. A. Al-Laham, C. Y. Peng, A. Nanayakkara, M. Challacombe, P. M. W. Gill, B. Johnson, W. Chen, M.W. Wong, C. Gonzalez and J. A. Pople, *Gaussian 03 (Revision C.02)*, Gaussian Inc, Wallingford, CT, 2004.

24 R. A. Kendall, F. H. Dunning Jr and R. J. Harrison, *J. Chem. Phys.*, 1992, **96**, 6796.

25 S. F. Boys and F. Bernardi, *Mol. Phys.*, 1970, **19**, 553.

26 F. Ugozzoli, *ABSORB Comput. Chem.*, 1987, **11**, 109.

27 A. Altomare, M. C. Burla, M. Camalli, G. Cascarano, C. Giacovazzo, A. Guagliardi and G. Polidori, SIR92, *J. Appl. Crystallogr.*, 1994, **27**, 435.

28 G. M. Sheldrick, SHELXL-97, *Program for Crystal Structure Refinement*, University of Göttingen, 1997, http://shelx.uni-ac.gwdg.de/shelx/index.html.

29 M. Nardelli, PARST97, updated version of PARST 95, *J. Appl. Crystallogr.*, 1995, **28**, 659.

